

The Potential to use Variations in Tree-Ring Geometric Center to Estimate Past Wind Speed Change

Keyan Fang (✉ kfang@fjnu.edu.cn)

Fujian Normal University

Maosheng He

Leibniz Institute of Atmospheric Physics at the Rostock University

Maowei Bai

Fujian Normal University

Zhipeng Dong

Fujian Normal University

Hans W. Linderholm

University of Gothenburg

Cesar Azorin-Molina

Spanish National Research Council

Zhengtang Guo

Chinese Academy of Sciences

Research Article

Keywords:

Posted Date: January 25th, 2022

DOI: <https://doi.org/10.21203/rs.3.rs-990762/v2>

License:   This work is licensed under a Creative Commons Attribution 4.0 International License.

[Read Full License](#)

Abstract

Tree radial growth is characterized by not only the annual ring-width increment but also shifts in the tree-ring geometric center (TRGC) if subjected to asymmetric external forcing, such as prevailing winds. Previous dendrochronological studies have used the asymmetric growth derived from tree-ring widths to reconstruct wind speed changes. Here we propose a novel method use quantitative TRGC measurements to estimate wind speed. We investigated TRGC shifts in northeast China, where the prevailing westerly winds are strong and persistent. We found that the TRGC showed significant correlations ($r = 0.64$, $p < 0.01$) with wind speed in May-September. The higher tree geometry sensitivity to wind speed obtained with the new method compared to previous ones, suggests the possibility of reconstructing historical wind change and variability in prevailing winds using TRGC. In addition, by correcting tree-ring radius according to their TRGC shifts, the basal area increment (BAI) was calculated. Our new BAI estimation provided stronger correlations with climate than both the standard tree-ring width chronology and a traditional BAI estimation. We suggest that future dendrochronological studies should consider TRGC shifts to increase the accuracy in climate reconstructions.

Introduction

Tree-ring data is due to its accurate dating, high climate sensitivity and wide distribution^{1,2} the most widely used high-resolution proxy for the reconstruction of past-millennium climate variables, such as air temperature³⁻⁶, hydroclimate⁷⁻⁹ and internal climate variability^{10,11}. These reconstructions provide a long-term context to evaluate current climate change. Thus, it is vital that the tree-ring data used faithfully reflects the annual growth responses of trees to climate.

When building a chronology, which is the base for further reconstructions, all ring widths from trees growing in a particularly year are averaged with the aim of reducing any growth disturbances from individual trees and strengthening climate signals^{12,13}. This method is based on the assumption that the annual increments (the tree rings) of a tree are concentric, and that any point around the circumference represents these equally well. In fact, trees often show asymmetric growth in different parts of the trunk¹⁴. For example, in response to force of gravity, tree rings in coniferous (broadleaf) species tend to be wider at the downslope (upslope) side than the opposite in order to keep the trees as vertical as possible, known as compression (tension) wood¹. Similarly, persistent, intense wind stress can also cause asymmetric growth of the trees, resulting in compression wood on the leeward side for coniferous trees¹⁵. Accordingly, previous studies have employed the asymmetric variations of tree-ring widths to reconstruct wind speed changes¹⁵⁻¹⁷. However, existing studies have lacked an accurate mathematical description of the asymmetric feature of tree derived from tree-ring cores^{18,19}. Here we provide a novel method to quantify the asymmetric growth of tree rings and investigate its relationships with wind speed changes.

Trees strive to maintain a circular shape even under gravity or wind stress, because a circle maximizes the cross area for a given perimeter according to the Isoperimetric Inequality²⁰. In addition, a cylinder-shaped trunk has the largest capacity, in comparison with other shapes, to maintain the upright position of a tree²¹. Thus, we hypothesize that trees tend to shift their tree-ring geometric center (TRGC) to have asymmetric growth in response to mechanical forcings. That is, the radial growth of trees can, in addition to ring-widths, be expressed by shifts in the TRGC. To assess this feature, we developed a method to detect the shifts in the TRGC, which was employed on wind stressed trees in Huanggangliang, northeast China. We assume that TRGC shift is sensitive better proxy for wind stress than previously used growth differences at the windward and leeward sides of trees¹⁵⁻¹⁷. In addition, we used to the TRGC shifts to make improved calculation of the tree basal area increment (BAI), which were compared with the traditional tree-ring-based BAI method²²⁻²³.

Results

Our methods can reasonably capture the TRGC shift of individual trees, as illustrated in Figure 1. The general westward shift of the TRGC can be attributed to the eastward pressure on the tree stems posed by the dominating westerlies in the study area. The TRGC showed considerable differences to the tree-ring difference index (TRDI) (Figure 2a; $r = 0.15$, $p > 0.05$), which expresses the differences between the tree-ring widths on the windward and leeward sides^{15,16}. The BAI series based on our new method showed a closer match ($r = 0.86$, $p < 0.01$) with the standard chronology (STD) than the BAI using traditional method (Figure 2b; $r = 0.42$, $p > 0.05$).

As shown in Figure 3a, the TRGC exhibited significant correlations with mean maximum wind speed during parts of the growing season in May ($r = 0.50$, $p < 0.05$), June ($r = 0.60$, $p < 0.01$) and September ($r = 0.56$, $p < 0.05$). The TRDI only showed significant correlations with mean maximum wind speed in September ($r = 0.59$, $p < 0.01$). Moreover, the TRGC showed stronger correlations with the average May-September mean maximum wind speed ($r = 0.64$, $p < 0.01$) than TRDI ($r = 0.31$, $p > 0.05$). Both TRGC and TRDI showed weaker correlations with air temperature, precipitation and PDSI than with mean maximum wind speed (Figure 3b, 3c and 3d).

The BAI measurements from both methods and the average ring-width chronology showed significant correlations with mean maximum wind speed, air temperature and precipitation in some months (Figure 4a, 4b and 4c). The BAI and tree-ring chronology showed more significant correlations with scPDSI than the other parameters (Figure 4d). The BAI based on the new method showed significant ($p < 0.05$) correlations with scPDSI from January to July. The STD also showed significant correlations with the scPDSI from January to May. While the BAI based on traditional method only show significant correlations with the scPDSI in January ($r = 0.45$, $p < 0.05$) and February ($r = 0.49$, $p < 0.05$). The BAI based on our new method showed stronger correlation ($r = 0.54$, $p < 0.05$) with the January-June mean scPDSI than the BAI based on traditional method ($r = 0.43$, $p < 0.05$).

The spatial correlation maps indicate a large area with significant ($p < 0.1$) correlations between the TRGC and mean zonal wind speed in May-September during the growing season but limited areas of significant correlations with the TRDI (Figure 5a and 5b). The new BAI showed significant ($p < 0.1$) correlations with the mean PDSI during the growing season in May-September for a larger area than the traditional BAI (Figure 5c and 5d). Taken together, our proposed TRGC showed stronger correlations with wind speed than the traditional TRDI and the BAI, according to the shift in TRGC showed stronger correlations with drought.

Discussion

TRGC changes in relation to wind speed. Previous studies assessing the influence of wind on asymmetric tree growth have calculated the residuals between the windward and leeward sides to reflect wind speed changes¹⁵⁻¹⁷. However, this method is limited when tracking changes in the dominant wind directions since it focuses on prescribed directions of the samples (windward and leeward). The TRGC method does not require prior knowledge about the dominant wind directions and should therefore to more accurately track any wind changes. Moreover, in response to asymmetric mechanical stress, trees shift the TRGC while maintain a circular shape. That is, the shift in TRGC is a direct response of asymmetric growth of the trees under mechanical forcings and is thus expected to be more sensitive to these forcings. This may explain why the TRGC shows stronger correlations with wind speed than the TRDI. The TRGC provides an alternative tree-ring proxy for wind speed reconstructions. Asymmetric growth of tree rings are often influenced by the distribution of roots and crown, as well as competitions from neighboring trees²⁴. For tree-ring based wind reconstruction, it is suggested to select trees with little disturbances from other factors. For example, trees near the forest boundary are less impacted by completion from other trees which are more common in the forest interior.

Improved BAI method based on changes in TRGC. Detrending raw tree-ring measurements is a basis and a challenging task in dendrochronology¹³. Trends in raw tree-ring measurement series include the biological trends and the geometric trends of a declining ring-width with the increase of the diameter of the tree, which are difficult to be separated. Some studies have employed BAI measurements rather than ring-width because this method can better simulate the geometric trend^{22,23}. However, existing BAI method assumes that tree rings grow in concentric circles, which is not accurate for many trees whose trunks are subjected to non-uniform growth stresses. Our new method considers the changes of the TRGC and radius of the tree ring, making more accurate than the old method. Since the new BAI method can better simulate the geometric changes of tree rings, it is readily understood that the improved BAI data shows stronger association with climate than traditional BAI.

Potential bias in climate reconstruction without considering changes in TRGC. The tree-ring width chronologies are usually developed as the mean of included tree-ring data, which are then used to reconstruct long-term climate change. Below, we demonstrate that the average of the tree-ring width in chronology development can be underestimated, if the shifts in TRGC caused increasing variances in tree-ring widths for cores of different directions.

As for the tree-ring width data, given that $n \gg 1$ tree cores were sampled from tree a and tree b , denoted as $\{a_1, a_2, \dots, a_n\}$ and $\{b_1, b_2, \dots, b_n\}$ and the annual area increments of the two trees are the same, i.e.,

$$\sum_{i=1}^n \frac{a_i^2}{n} = \sum_{i=1}^n \frac{b_i^2}{n}.$$

Given that the mean of the cores of tree a is \bar{a} and tree b is \bar{b} , but tree a has larger growth differences as indicated by larger variance than tree b , i.e.

$$\begin{aligned} \sum_{i=1}^n \frac{(a_i - \bar{a})^2}{n} &> \sum_{i=1}^n \frac{(b_i - \bar{b})^2}{n}. \leftarrow \\ \sum_{i=1}^n \frac{a_i^2}{n} + \sum_{i=1}^n \frac{\bar{a}^2}{n} - \sum_{i=1}^n \frac{2a_i\bar{a}}{n} &> \sum_{i=1}^n \frac{b_i^2}{n} + \sum_{i=1}^n \frac{\bar{b}^2}{n} - \sum_{i=1}^n \frac{2b_i\bar{b}}{n} \\ \bar{a}^2 - \sum_{i=1}^n \frac{2a_i\bar{a}}{n} &> \bar{b}^2 - \sum_{i=1}^n \frac{2b_i\bar{b}}{n}. \leftarrow \\ -\bar{a}^2 &> -\bar{b}^2. \leftarrow \end{aligned}$$

This indicates $\bar{a} < \bar{b}$.

That is, the average of tree-ring width can be higher for the trees with larger asymmetric growth than the trees with more even growth patterns. This highlights the need to consider growth differences in different directions of a tree due to shifts in TRGC, as it can bias tree-ring chronologies.

Methods

Dendrochronological methods. For each sampled *Picea koraiensis* Nakai tree, cores were taken from four directions, west, east, northwest and southeast, in a horizontal cross-section at breast height. The sampling directions were designed to track the main influences of wind stress from the westerlies in the study area. Cores that did not reach the pith or with injuries or branches were excluded, and in total, we obtained 182 cores from 38 trees. The tree-ring cores were air-dried, mounted and polished²⁵. The exact calendar year was assigned to each tree ring using the cross-dating procedure²⁶, and the dated cores were then measured with a 0.001 mm resolution. Most raw tree-ring measurements generally showed an upward growth trends, since the trees were still in their juvenile period (herein, the mean length of the trees is 23 years) where growth is generally increasing¹. Thus, we did not remove the age-related growth trends in the raw measurements by fitting negative exponential curves to generate a standard chronology²⁷, which is a common procedure for longer-lived trees. Instead, we generated a tree-ring chronology from the robust mean of the raw measurements²⁷.

TRGC detection and improved BAI methods. We herein propose a novel method to quantify the annual variations of the distances and orientations of the TRGC in a stem cross section with at least three cores

reaching the pith with known cross-angles between them. Assuming that N cores, sampled through the method specified in Section 2.2, intersect at the tree pith O , we can define θ_{ij} ($i, j=1,2,\dots,N$) as the cross angle between the i -th and j -th cores, and $\rho_j(t)$ denoting the distance between O and the tree ring of a given year t on the j -th core. Then $[\rho_j(t), \theta_{1j}]$ is the coordinate of the tree ring in a polar coordinate system where to the first core is referred to as the polar axis and O as the pole. $\mathbf{r}_j(t)=[x_j(t), y_j(t)]:=[\rho_j(t)\cos(\theta_{1j}), \rho_j(t)\sin(\theta_{1j})]$ defines the coordinates in a Cartesian coordinate system. When $N \geq 3$, $x_j(t)$ and $y_j(t)$ can be used for determining parameters of the circle equation $(x_j - a_t)^2 + (y_j - b_t)^2 = R_t^2$ through a least-square fit. The fitted a_t and b_t are the TRGC coordinates in the Cartesian system and R_t is the radius. Further, we calculated the $BAI_t = \pi \times (R_t^2 - R_{t-1}^2)$, where $t-1$ denotes the year before t .

Compared to traditional BAI estimation, which entail the assumption of concentric annual tree-ring increments^{22,23}, our BAI estimation takes the TRGC shift into account and should therefore be more reliable. The reliable portions of the tree-ring chronologies, the mean of the series of the TRGC and the BAI series, were those with sufficient sample size, here determined when the sub-sample signal strength (SSS) statistics reached above 0.80²⁸. The program for quantifying the TRGC is shown in the supplementary materials. Similar to ring-widths, BAI series generally show strong increasing trends in tree juvenile periods^{22,23}. Accordingly, we removed the linearly increasing BAI trend in the juvenile period.

Study Region And Data Availability

Study region. The study site was located on the Huanggangliang Mountain (43.5 °N; 117.5 °E; 1,935 m a.s.l.), in Chifeng City jurisdiction in Inner Mongolia, northeastern China (Figure 6a). Huanggangliang Mountain is a peak in the Greater Khingan Range, which extends 1,200 kilometers from north to south in northeastern China, dividing the Inner Mongolia Plateau and the Northeast Plain of China. The mountain is located on the boundary between the Asian summer monsoon area and the forest-steppe ecotone²⁹, with peak air temperatures and precipitation in summer¹⁶. The westerly winds dominate the study area, with an annual mean wind speed of $\sim 3.8 \text{ m s}^{-1}$, making it ideal for detecting impacts of wind stress on trees. The sampling site was situated on a mountain top with flat topography on which an open *Picea koraiensis* Nakai forest grow (Figure 6b). Samples were taken from the western boundaries of the forests, where the trees were assumed to be strongly impacted by winds (Figure 6c).

Declarations

Acknowledgements

We acknowledge supports from the Strategic Priority Research Program of the Chinese Academy of Sciences (XDB26020000), the Swedish Formas project (2017-01408), the National Science Foundation of China (41822101, 41971022, 41888101 and 41772180), fellowship for Youth Talent Support Program of

Fujian Province and the innovation team project (IRTL1705). C.A.M. was supported by Ramon y Cajal fellowship (RYC-2017-22830) and the grant no. RTI2018-095749-A-I00 (MCIU/AEI/FEDER, UE).

Author Contributions

K. F. designed the study, conducted the analyses and wrote the manuscript. M.H., M.B. and Z.D. contributed to sample collection, data analyses, figure production and manuscript preparation. H.W.L., C.A.-M. and Z.G. discussed and revised the manuscript.

Statement

The collection of tree ring samples was approved by the competent unit of Chifeng City, Inner Mongolia Autonomous Region.

Data availability. Our tree-ring samples collection comply with the China meteorological industry standard: code for sampling tree rings for climatic studies of tree rings (standard number: QX/T 90-2008, China standard classification No. A 47, <http://hbba.sacinfo.org.cn/stdDetail/7d8e451ff61b29671a81ec2c818c895a>). The tree ring samples of *Picea koraiensis* Nakai were stored in the tree ring laboratory (Figure 6d), Fujian Normal University, China. Professor Fang K.Y. was in charge of the laboratory. Monthly mean air temperature (in °C), precipitation (in mm), and maximum wind speed (m s^{-1}) from Xilinhot, the closest meteorological station (Figure 6a, 116.07 °E, 43.57 °N; 1,003 m a.s.l.), were obtained from the China Meteorological Administration (CMA; <http://www.nmic.gov.cn/>) for 1998-2018. The monthly mean maximum wind speed data was calculated from the mean of the daily maximum wind speed data, and the directions were according to those most frequent in the daily maximum wind speed data. The wind speed data were previously homogenized and quality controlled³⁰ to avoid potential biases from, for example, shifts in station locations³¹ and anemometer aging³². We also compared our tree-ring data with wind speed at 850 hPa (corresponding to ~1500 m a.s.l.) from the European Centre for Medium-Range Weather Forecasts (ECMWF) ERA5 reanalysis dataset³³ spanning from 1979 to nowadays. The self-calibrated Palmer Drought Severity Index (scPDSI) data is calculated from available air temperature and precipitation data from 1850 to 2018 at a 2.5° grid system to estimate the dryness in regions of different drought regimes³⁴⁻³⁶. We used the scPDSI from the nearest grid point (118.75 °E, 43.75 °N) to compare with our tree-ring data.

References

1. Fritts, H.C. *Tree rings and climate* (Academic Press 1976).
2. Hughes, M.K., Swetnam, T.W. & Diaz, H.F. *Dendroclimatology: progress and prospects* (Springer 2011).
3. Neukom, R., Steiger, N., Gómez-Navarro, J.J., Wang, J.H. & Werner, J.P. No evidence for globally coherent warm and cold periods over the preindustrial Common Era. **571**, 550–554 (2019).
4. PAGES 2k Consortium. Continental-scale temperature variability during the past two millennia. *Geosci.* **6**, 339–346 (2013).

5. Stocker, T.F. et al. Climate change 2013: the physical science basis. Intergovernmental panel on climate change, working group I contribution to the IPCC fifth assessment report (AR5) (Cambridge University Press 2013).
6. Zhang, P. et al. Abrupt shift to hotter and drier climate over inner East Asia beyond the tipping point. *Science* 370, 1095–1099 (2020b).
7. Cook, E.R. et al. Old world megadroughts and pluvials during the common era. *Sci. Adv.* 1, 1–9 (2015).
8. Fang, K.Y., et al. Drought variation of western Chinese loess plateau since 1568 and its linkages with droughts in western North America. *Clim. Dynam.* doi: 10.1007/s00382-00017-03545-00389 (2018).
9. Ljungqvist, F.C. et al. Northern hemisphere hydroclimate variability over the past twelve centuries. *Nature*. 523, 94-98; doi:10.1038/nature17418 (2016).
10. Fang, K.Y., et al. Oceanic and atmospheric modes in the Pacific and Atlantic oceans since the Little Ice Age (LIA): towards a synthesis. *Quaternary Sci. Rev.* 215, 293–307 (2019).
11. Wang, J.L. et al. Internal and external forcing of multidecadal Atlantic climate variability over the past 1,200 years. *Nat. Geosci.* doi: 10.1038/NGEO2962 (2017).
12. Cook, E.R. & Kairiukstis, L. *Methods of dendrochronology* (Kluwer Academic Press, 1990).
13. Hughes, M.K., Swetnam, T.W. & Diaz, H.F. *Dendroclimatology: progress and prospects* (Springer 2011).
14. Harmon, M.H. A study of some factors affecting asymmetrical growth of trees. *Butler University Botanical Studies* 5, 134–144 (1942).
15. Wade, J.E. & Hewson, E.W. Trees as a local climatic wind indicator. *J. Appl. Meteorol.* 18, 1182–1187 (1979).
16. Fang, K.Y., et al. Tree growth differences from the windward and leeward sides reflect wind stress in northeastern Inner Mongolia. *Dendrochronologia* (under review) (2021).
17. Tomczak, A., Jelonek, T., Grzywiński, W., Mania, P. & Pazdrowski, W. The effects of wind exposure on Scots pine trees: within-stem variability of wood density and mechanical properties. *Forests* 11, 1095 (2020).
18. Bakker, J.D. A new, proportional method for reconstructing historical tree diameters. *Can. J. Forest Res.* 35, 2515–2520 (2005).
19. Biondi, F. From dendrochronology to allometry. *Forests* 11, 146 (2020).
20. Osserman, R. The isoperimetric inequality. *B. Am. Math. Soc.* 84, 1182-1238 (1978).
21. Dugas, R. *A history of classical mechanics* (Dover Publications Inc 2011).
22. Biondi, F. & Qeadan, F. A theory-driven approach to tree-ring standardization: defining the biological trend from expected basal area increment. *Tree Ring Res.* 64, 81–96 (2008).
23. Monserud, R.A. & Sterba, H. A basal area increment model for individual trees growing in even- and uneven-aged forest stands in Austria. *Forest Ecol. Manag.* 80, 57–80 (1996).

24. Harmon, M.H. A study of some factors affecting asymmetrical growth of trees. *Butler University Botanical Studies* 5, 134–144 (1942).
25. Stokes, M.A., Smiley, T.L. *An introduction to tree-ring dating* (University of Chicago Press 1968).
26. Holmes, R.L. Computer-assisted quality control in tree-ring dating and measurement. *Tree-ring bull* 43, 69–78 (1983).
27. Cook, E.R. *A time series analysis approach to tree ring standardization* (The University of Arizona 1985).
28. Wigley, T.M.L., Briffa, K.R. & Jones, P.D. Average value of correlated time series, with applications in dendroclimatology and hydrometeorology. *J. Appl. Meteorol. Clim.* 23, 201–234 (1984).
29. Chen, F.H. et al. Westerlies asia and monsoonal asia: spatiotemporal differences in climate change and possible mechanisms on decadal to sub-orbital timescales. *Earth-Sci. Rev.* 192, 337–354 (2019).
30. Zhang, G.F., Azorin-Molina, C., Chen, D.L., Guijarro, J.A. & Shi, P.J. Variability of daily maximum wind speed across China, 1975- 2016: An examination of likely causes. *J. Climate* 33, 2793–2816 (2020a).
31. Wan, H., Wang, X.L. & Swail, V.R. Homogenization and trend analysis of Canadian near-surface wind speeds. *J. Climate.* 23, 1209–1225 (2010).
32. Azorin-Molina, C. et al. Evaluating anemometer drift: A statistical approach to correct biases in wind speed measurement. *Atmos. res.* 203, 175–188 (2018).
33. Hersbach, H., Bell, B., Berrisford, P., Hirahara, S. & Thépaut, J. The ERA5 global reanalysis. *Quarterly Journal of the Royal Meteorological Society* 146, 1999–2049 (2020).
34. Dai, A., Trenberth, K.E. & Qian, T. A global dataset of palmer drought severity index for 1870-2002: relationship with soil moisture and effects of surface warming. *J. Hydrometeorol.* 5, 1117–1130 (2004).
35. Palmer, W.C. *Meteorological drought* (Washington, D.C. 1965).
36. Wells, N., Goddard, S. & Hayes, M.J. A self-calibrating palmer drought severity index. *J. Climate* 17, 2335–2351 (2004).

Figures

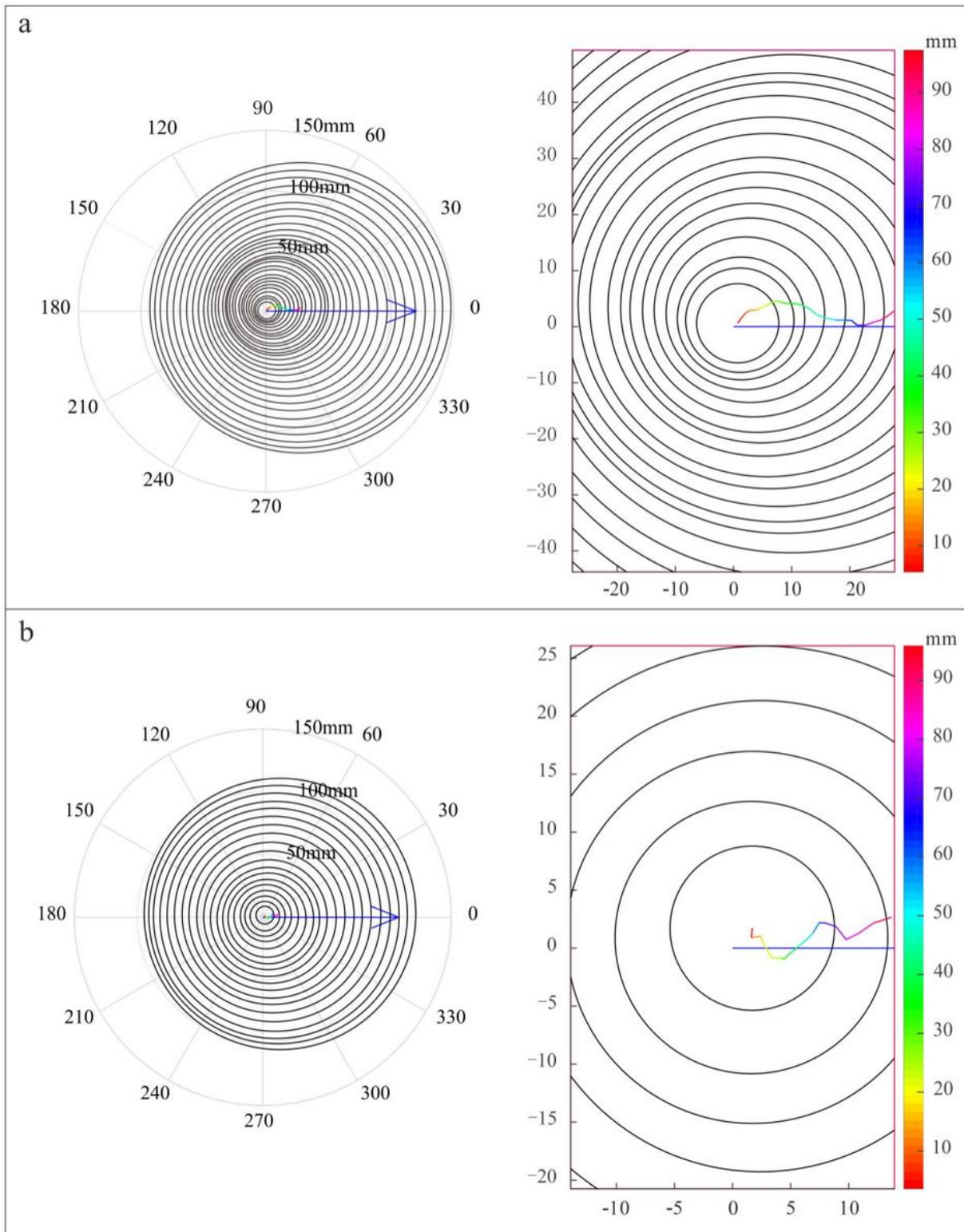


Figure 1

Examples of the annual changes of the tree-ring geometric center (TRGC) using the proposed methods.

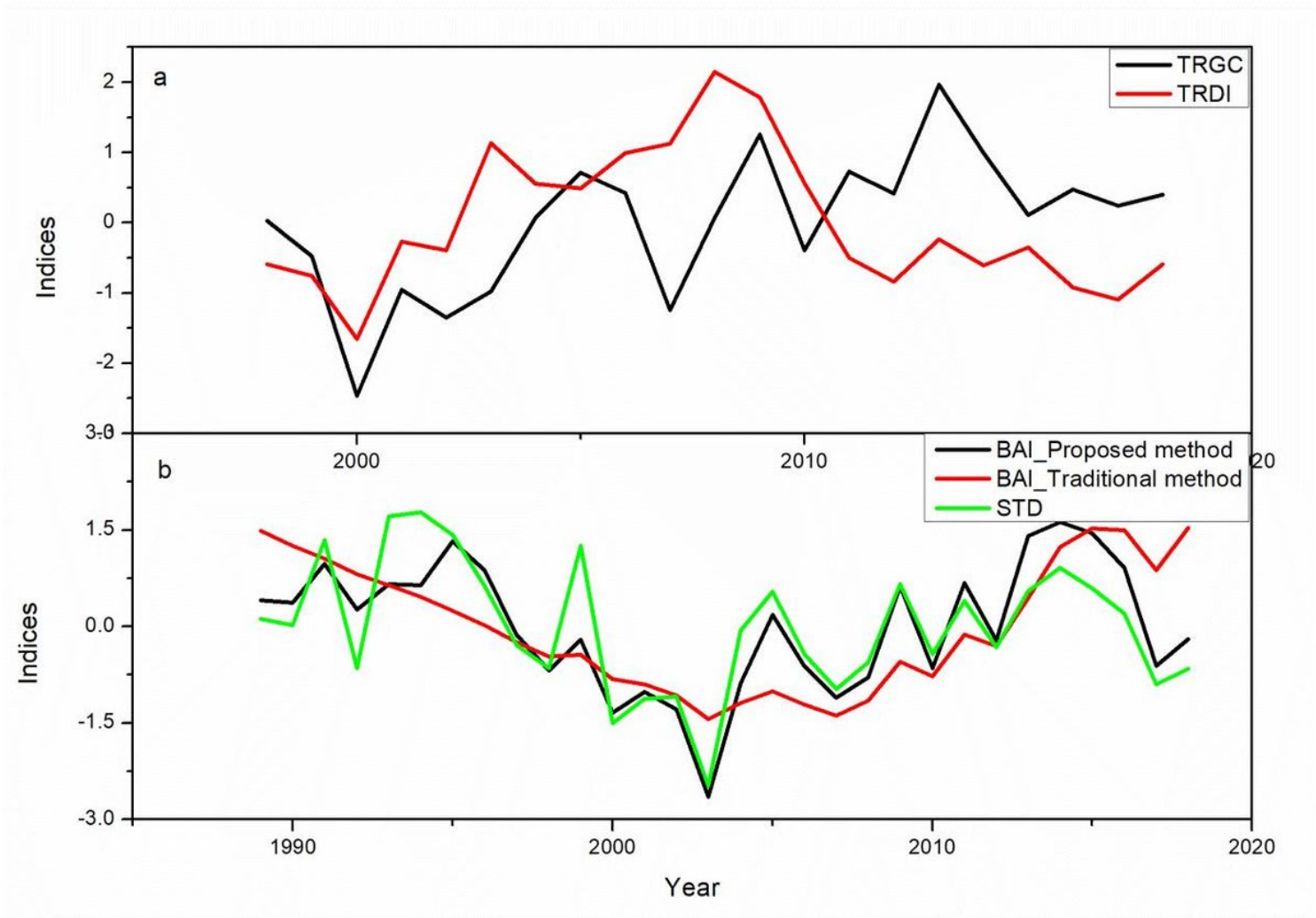


Figure 2

Comparisons between the (a) variations of the tree-ring geometric center (TRGC) and the tree-ring difference index, and between (b) basal area increments (BAI) based on proposed and traditional methods and the standard chronology (STD).

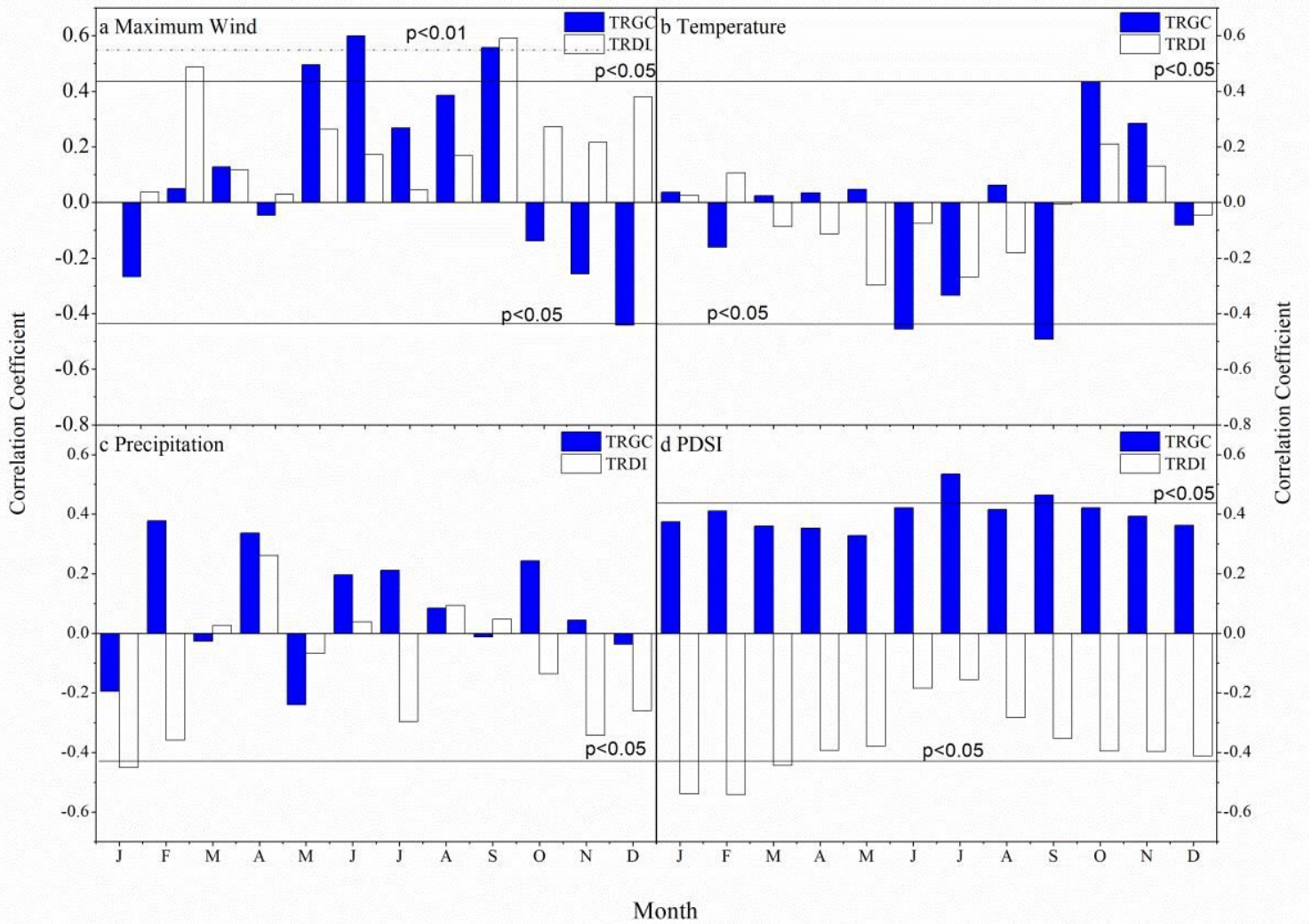


Figure 3

Correlations between the tree-ring geometric center (TRGC) and tree-ring difference index (TRDI) and the monthly (a) mean maximum wind speed, (b) temperature, (c) precipitation and (d) Palmer Drought Severity Index (PDSI) from January to December.

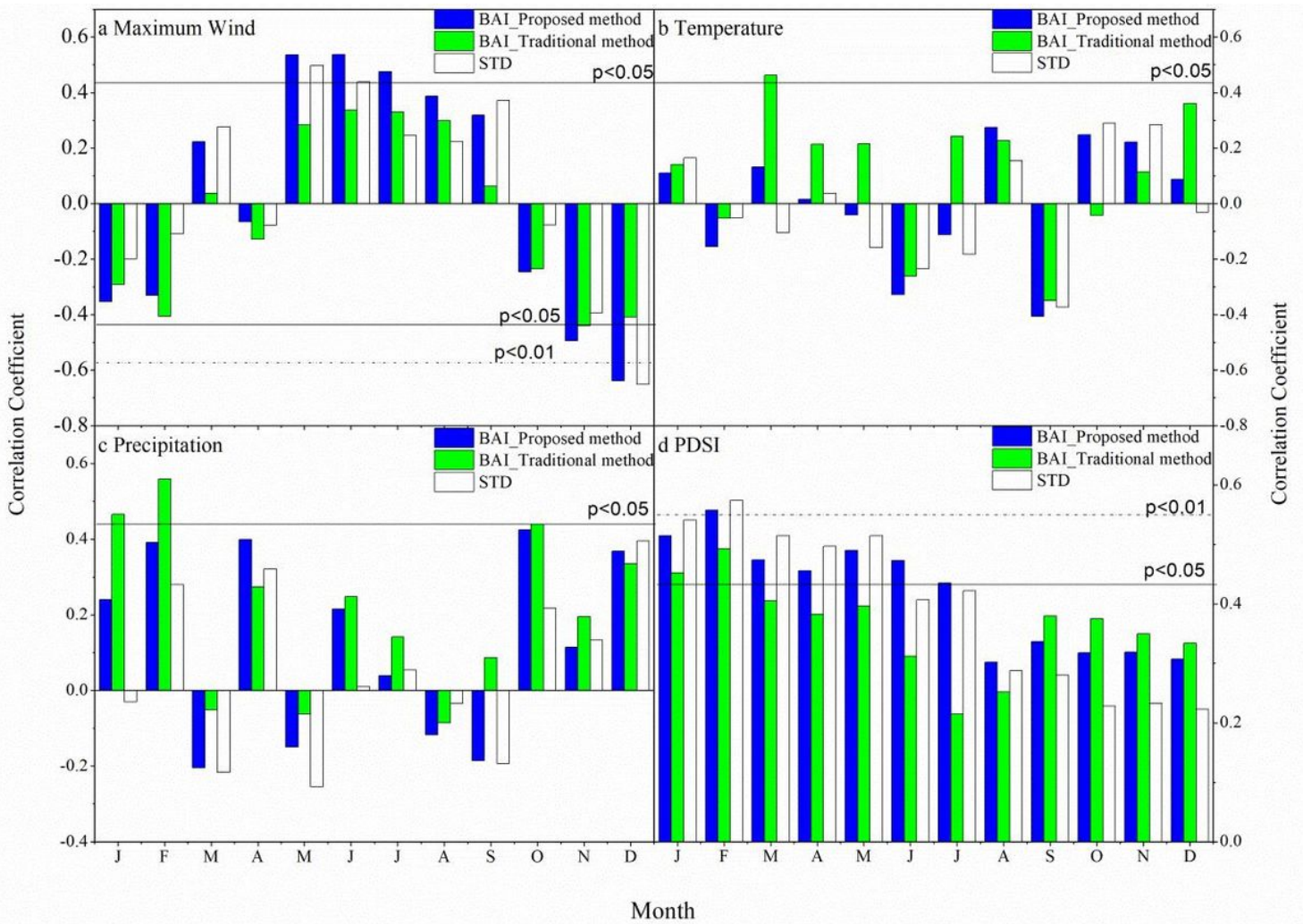


Figure 4

Correlations between basal area increments (BAI) based on proposed and traditional methods and the standard chronology (STD) and the monthly (a) mean maximum wind speed, (b) temperature, (c) precipitation and (d) Palmer Drought Severity Index (PDSI) from January to December.

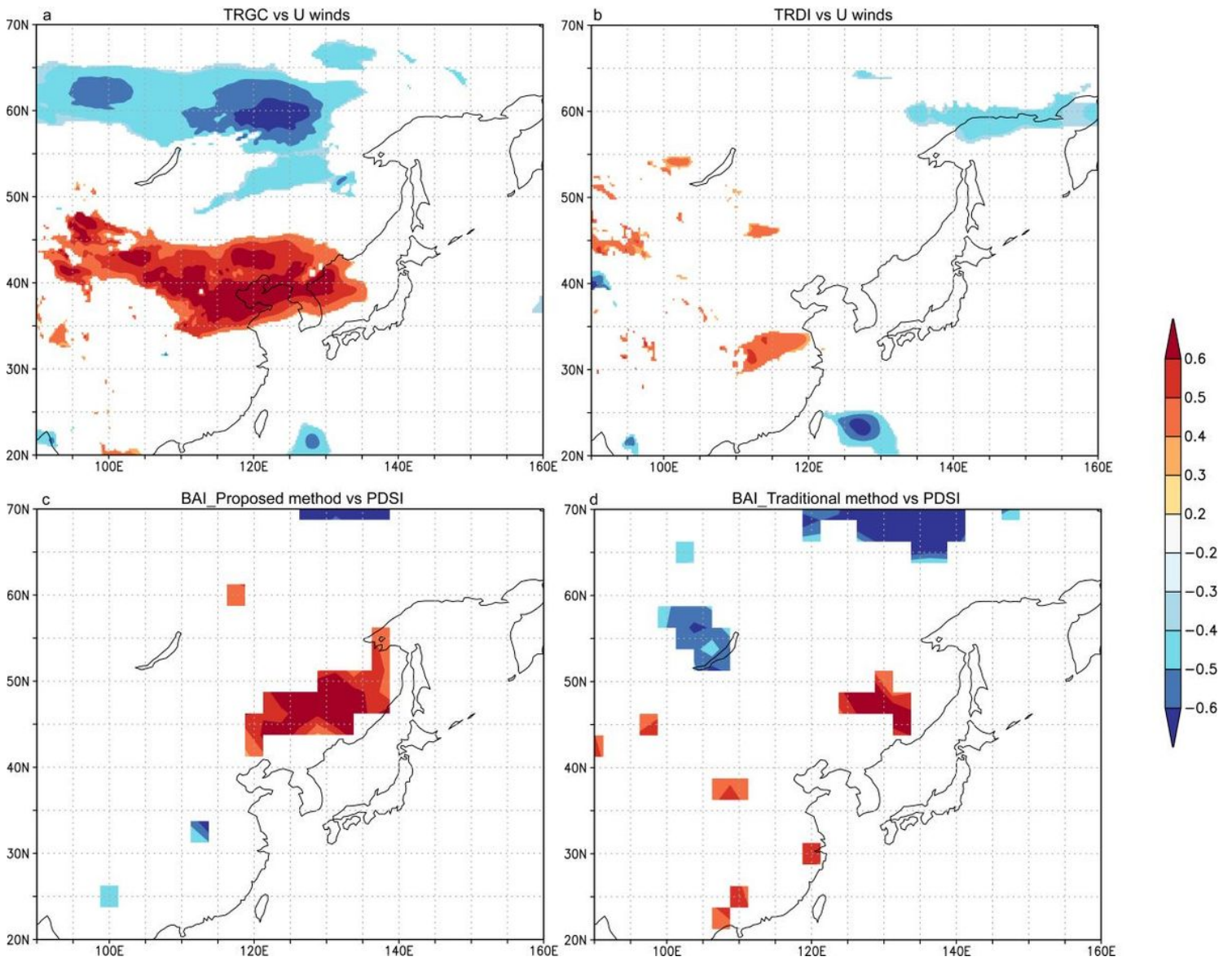


Figure 5

Correlations between the (a) tree-ring geometric center (TRGC) and (b) tree-ring difference index (TRDI) instrumental winds and the zonal wind speed (U winds) during the growing season of May-September, as well as between basal area increments (BAI) based on the (c) proposed and (d) traditional methods and the May-September Palmer Drought Severity Index (PDSI).

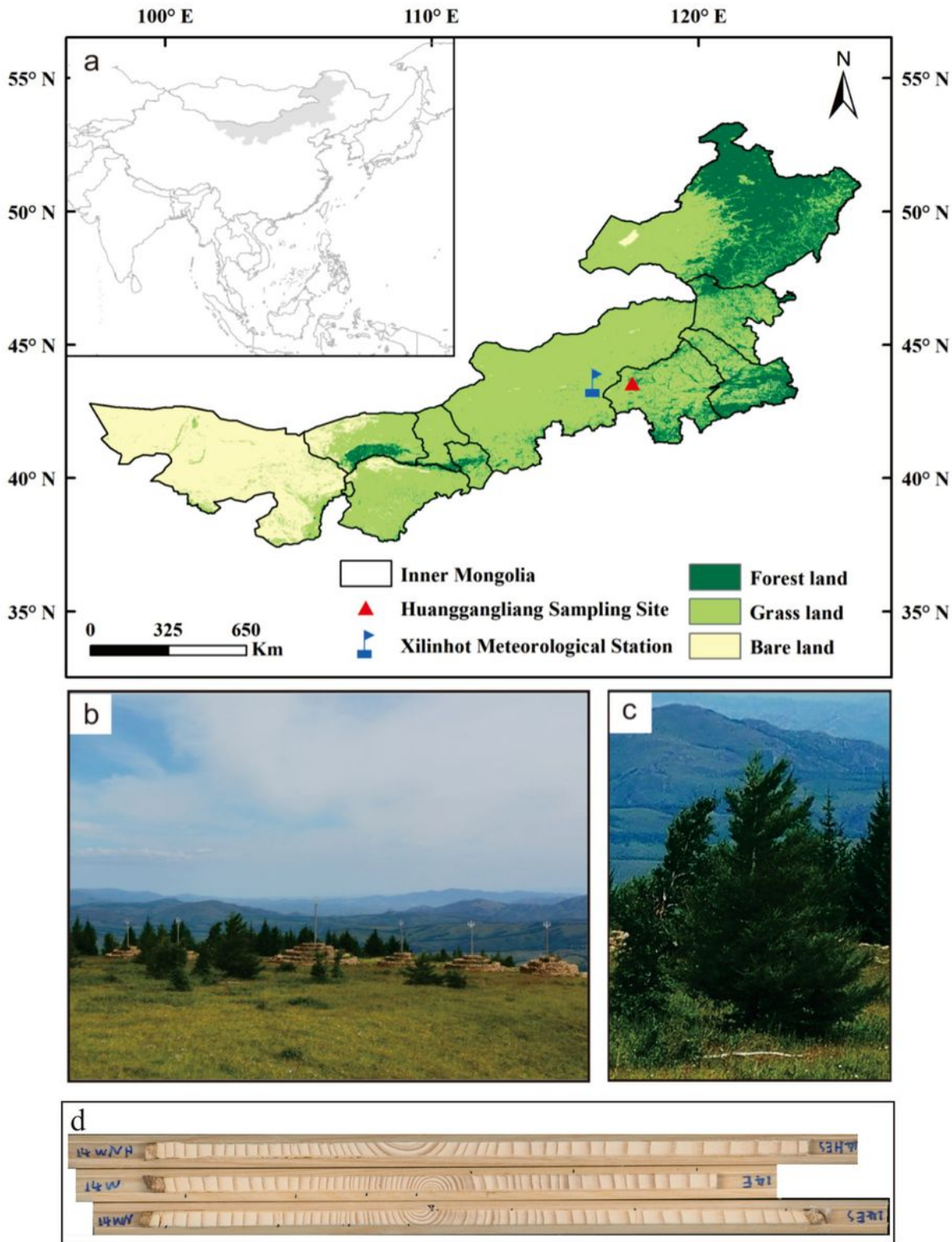


Figure 6

(a) Locations of the Huanggangliang sampling site and the meteorological station in northeastern Inner Mongolia and study region in central and eastern Asia and the (b) photo of the sampling site at the boundary of the forest on the plateau of the mountain top, the (c) photo of a sampled tree under wind stress, and the (d) photo of tree-ring sample cores of *Picea koraiensis* Nakai (provided by Mei Z.P.).

Supplementary Files

This is a list of supplementary files associated with this preprint. Click to download.

- [CircleParaLS.pdf](#)
- [CircleParaLSd1.pdf](#)